Inunicosides A−K, rare polyacylated *ent*-kaurane diterpenoid glycosides from the flowers of *Inula japonica*

Zhi-Pu Yu, Jin-Hai Yu, Jun-Sheng Zhang, Shu-Juan Yu, Hua Zhang

PII: S0040-4020(19)31118-4

DOI: https://doi.org/10.1016/j.tet.2019.130732

Reference: TET 130732

To appear in: *Tetrahedron*

Received Date: 11 August 2019

Revised Date: 28 September 2019

Accepted Date: 22 October 2019

Please cite this article as: Yu Z-P, Yu J-H, Zhang J-S, Yu S-J, Zhang H, Inunicosides A−K, rare polyacylated *ent*-kaurane diterpenoid glycosides from the flowers of *Inula japonica*, *Tetrahedron* (2019), doi: https://doi.org/10.1016/j.tet.2019.130732.

Graphical abstract:

Inunicosides A–K, rare polyacylated *ent*-kaurane diterpenoid glycosides from the flowers of *Inula japonica*

Zhi-Pu Yu, Jin-Hai Yu, Jun-Sheng Zhang, Shu-Juan Yu, Hua Zhang

Inula japonica

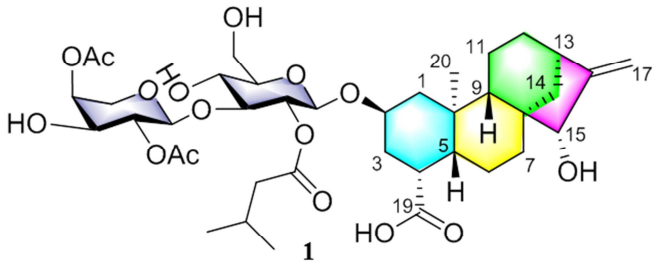

Enzymatic hydrolysis

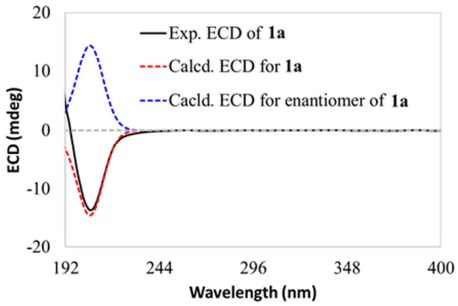

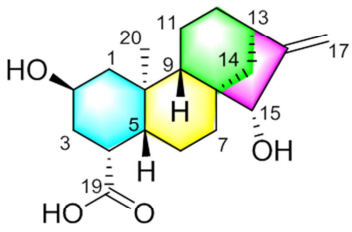

1a (2*R*,4*R*,5*R*,8*R*,9*S*,10*R*,13*R*,15*S*)

Inunicosides A–K, rare polyacylated *ent*-kaurane diterpenoid glycosides from the flowers of *Inula japonica*

Zhi-Pu Yu,[a,b] Jin-Hai Yu,[b] Jun-Sheng Zhang[b], Shu-Juan Yu[a,b], Hua Zhang[b,*]

[a]*School of Chemistry and Chemical Engineering, University of Jinan, 336 West Road of Nan Xinzhuang, Jinan 250022, China*

[b]*School of Biological Science and Technology, University of Jinan, 336 West Road of Nan Xinzhuang, Jinan 250022, China*

*Corresponding author

E-mail address: bio_zhangh@ujn.edu.cn (H. Zhang).

ORCID

Hua Zhang: 0000-0002-5959-6473

ABSTRACT

Inunicosides A–K (1–11), eleven unusual polyacylated *ent*-kaurane diterpenoid glycosides, were isolated from the flowers of a traditional Chinese herbal plant *Inula japonica*. Their structures with absolute configurations were determined on the basis of comprehensive spectroscopic analyses, chemical degradation, enzymatic hydrolysis and ECD experiments. Among these isolates, inunicoside K (**11**) showed mild antibacterial activity against *Staphylococcus aureus* ATCC 25923. Diterpene constituents have been rarely reported in the *Inula* species, and thus the discovery of this panel of compounds greatly enriches the chemical diversity of metabolites from the genus *Inula*.

Keywords: Compositae; *Inula japonica*; *ent*-kaurane; diterpenoid glycoside; polyacylation; antibacterial

1. Introduction

The genus *Inula* (family Compositae) comprises about 100 species widely distributed on the continents of Europe, Africa and Asia, particularly around the Mediterranean area [1]. Over 20 species and a number of variants grow in China, with several ones such as *I. britanica* and *I. japonica* being widespread species [1]. *Inula* is an important tribe of medicinal plants, among which *I. japonica* is well known in traditional Chinese medicine and its dried capitula have long been used under the name 'Xuanfuhua' for the treatment of cough, phlegm and related symptoms [2]. The plant *I. japonica* is very famous in the natural products field, especially for its abundant and diverse sesquiterpenoid constituents, *e.g.* eudesmane, germacrane and guaiane types, with monomers, dimers and even trimers [3-8]. In addition, four rare diterpenoid glycosides were also reported from this herb [9].

During the course of our research to explore new bioactive molecules from Chinese traditional herbs, the flower buds of *I. japonica* were phytochemically studied in the current work. Apart from the well-investigated sesquiterpenoid compounds [10], new interesting chemical constituents were also detected in the most polar fractions generated from the EtOAc partition of the ethanol extract. Subsequently, an intensive fractionation of these polar fractions led to the separation of a panel of diterpenoid glycosides. Through a combination of various means including MS, NMR, ECD, chemical hydrolysis and enzymatic degradation, these compounds were identified to be ten new 18-nor-*ent*-kaurane diterpenoid glycosides (**1–10**) with a 4-carboxyl group and a disaccharide moiety of glucose and arabinose at C-2, a new intact *ent*-kaurane diterpenoid glycoside (**11**) with 4-geminal carboxyl groups and the same sugar connection as **1–10**, and a known diterpenoid glycoside analogue (**12**) [11]. The *in vitro* cytotoxicity (MDA-MB-231 & HeLa), NO release inhibition (in RAW264.7 macrophages) and antibacterial (*Staphylococcus aureus* & b*Bacillus subtilis*) activities of all the isolates were evaluated in the current work. Moreover, their acetylcholinesterase (AChE), α-glucosidase and pancreatic lipase inhibitory activities were also tested. Details of the isolation, structure characterization and biological evaluations of these glycosides are described below.

2. Results and discussion

Compound **1**, a white amorphous powder, was assigned a molecular formula of $C_{39}H_{58}O_{16}$ based on its (+)-HRESIMS (*m/z* 805.3607 $[M + Na]^+$, calcd 805.3617) and ^{13}C NMR data, corresponding to 11 indices of hydrogen deficiency. The ^1H NMR data (Table 1) showed two doublet signals at δ_H 4.60 (d, J = 8.0 Hz) and 4.46 (d, J = 6.6 Hz) diagnostic of two sugar anomeric protons, which along with the corresponding carbon resonances at δ_C 99.0 and 100.7 suggested the presence of two monosaccharide units. Further analyses of the ^1H–^1H COSY, HSQC and HMBC data (Fig. 2A) unambiguously assigned all their NMR signals as shown in Tables 1 and 2, based on which the two sugars were determined be one glucopyranose and one arabinopyranose, with β- and α-configurations for the two anomeric carbons being determined via the coupling constants of anomeric protons (8.0 Hz for glucopyranose and 6.6 Hz for arabinopyranose), respectively [12,13]. The assignments of D-glucose and L-arabinose were established via HPLC comparison of their (*S*)-(−)-1-phenylethylamine derivatives with those of authentic standard sugar samples (Fig. S95, supporting information (SI)). In addition, the key HMBC correlation (Fig. 2A) from H-1″ (δ_H 4.46) to C-3′ (δ_C 83.4) established the connection between the two sugar moieties as shown. Characteristic signals for one isovaleryloxy [δ_H 2.24, 2.21, 2.11, 0.99, 0.98; δ_C 171.4, 43.7, 25.8, 22.8 (2C)] and two acetoxy [δ_H 2.11 (s) and δ_C 21.0, 171.2; δ_H 2.15 (s) and δ_C 21.2, 170.8] groups were also evident from the NMR data, and they were assigned to locate at C-2′, C-2″ and C-4″ by the pivotal HMBC correlations from H-2′ (δ_H 4.94), H-2″ (δ_H 4.95) and H-4″ (δ_H 5.06) to the corresponding ester carbonyl carbons, respectively.

Besides those for the disaccharide moiety, the NMR data for **1** also displayed typical signals for a carboxyl group (δ_C 179.3), an exocyclic terminal double bond (δ_H 5.21, 5.08; δ_C 160.0, 108.9), two sp^3 oxymethines (δ_H 3.80, 4.23; δ_C 82.8, 71.3) and a singlet methyl (δ_H 0.97; δ_C 16.9). The aforementioned data accounted for seven indices of hydrogen deficiency, and the remaining four supported a tetracyclic scaffold for the aglycone part of **1**. Comprehensive analyses of 2D NMR data (Fig.

2A) confirmed the planar structure for the aglycone of **1** as drawn, incorporating a kaurane or *ent*-kaurane type diterpenoid skeleton. In detail, two spin-spin coupling systems [**a** (H_2-1 to H_2-7) and **b** (H-9 via H_2-11 to H_2-14), see Fig. 2A] as shown in bold bonds were readily built up via examination of the ^1H–^1H COSY data. The HMBC correlations from H_3-20 to C-1 (δ_C 47.3), C-5 (δ_C 49.3), C-9 (δ_C 52.7) and C-10 (δ_C 40.8), H_2-7 to C-8 (δ_C 47.8) and C-9, and H-9 to C-8 (Fig. 2A), along with fragment **a**, established rings A and B as depicted. Subsequently, the HMBC correlations from H-9 to C-8 and C-14 (δ_C 36.4), in combination with fragment **b**, assembled ring C, and ring D was then constructed via the HMBC interactions from H_2-17 to C-13 (δ_C 42.4), C-15 (δ_C 82.8) and C-16 (δ_C 160.0), and H-15 to C-7, C-8 and C-14. Furthermore, the presence of 15-OH was confirmed by the chemical shifts of C-15 (δ_C 82.8) and H-15 (δ_H 3.80). Finally, the HMBC correlations from H-1′ to C-2 (δ_C 71.3), and H_2-3, H-4 and H-5 to C-19 (179.3), attached the disaccharide moiety and the carboxyl group at C-2 and C-4, respectively.

The relative configuration for the aglycone unit of **1** was established by interpretation of the ROESY data (Fig. 2B). The strong interactions of H_3-20 with H-2, H-6α (δ_H 1.91), H-12α (δ_H 1.57) and H-14α (δ_H 1.86) indicated that they were on the same side of the molecule and were assigned to be α-oriented, with ring D being disposed on top of ring C as shown in Fig. 2B. Accordingly, the correlations of H-5 with H-3β (δ_H 1.18), H-4, H-7β (δ_H 1.43) and H-9, H-3β with H-1β (δ_H 0.76), and H-9 with H-15, revealed that they were on the other side and β-directed, thus leaving 4-CO_2H and 15-OH α-bonded. Subsequent hydrolysis of **1** with snailase afforded the aglycone (**1a**), and it was identified to be atractyligenin (Table S4 and Figs. S96–S98, SI) whose absolute configuration had been previously established via single-crystal X-ray diffraction analysis [14]. Furthermore, the theoretical ECD spectrum of the aglycone (atractyligenin) was also acquired by TD-DFT (time-dependent density functional theory) method and matched the experimental one perfectly (Fig. 3). It was interesting to note that the ECD curve of **1** was also highly consistent with that of the aglycone (**1a**, Fig. 3), indicating that the sugar part contributed little or even no effect

to the ECD data. Therefore, compound **1** was unambiguously elucidated as an 18-nor-*ent*-kaurane type diterpenoid glycoside and it was named inunicoside A.

Compound **2** displayed an ammonium adduct ion peak at *m/z* 842.4188 (calcd 842.4169) in the (+)-HRESIMS analysis, which together with the ^{13}C NMR data suggested a molecular formula of $C_{41}H_{60}O_{17}$, with 42 mass units more than that of **1** and suggestive of an extra acetyl group. Comparison of the NMR data (Tables 1 and 2) for **2** with those of **1** revealed that they were structural analogues, with the only difference occurring to the glucopyranosyl moiety, whose H_2-6′ signals (δ_H 4.44, 4.24) were remarkably downfield shifted as compared with those (δ_H 3.93, 3.76) for **1**. In addition, the appearance of NMR resonances for an additional acetoxyl group (δ_H 2.05; δ_C 21.1, 171.2) implied that the 6′-OH in **2** was acetylated, and this was further confirmed by the HMBC correlations from H_2-6′ to the newly introduced acetyl carbonyl carbon. Detailed examination of the full 1D and 2D (Figs. S10–S15, SI) NMR data for **2**, especially of key proton-proton couplings, HMBC and ROESY correlations, established the gross structure of **2** as drawn (Fig. 1) and also corroborated the relative configuration of **2** to be identical with that of **1**. Compound **2** was thus structurally characterized as the 6′-*O*-acetyl derivative of **1** and was named inunicoside B.

Compounds **3** (inunicoside C) and **4** (inunicoside D) were assigned the same molecular formula of $C_{41}H_{60}O_{17}$ as **2**, which was evidenced by their (+)-HRSEIMS ion peaks at *m/z* 842.4193 and 842.4183 (both $[M + NH_4]^+$, calcd 842.4169), respectively, as well as the ^{13}C NMR data. Analysis of the NMR data (Tables 1 and 2) for **3** confirmed that it was isomeric with **2**, and the only difference between the two cometabolites was attributed to the acetylation position within the arabinopyranosyl fragment. Compared with those of **2**, H-3″ (δ_H 4.89) of **3** was significantly downfield shifted while H-4″ (δ_H 4.07) of **3** was observed in the normal range, suggesting that the 3″-OH in **3** instead of the 4″-OH in **2** was acetylated. This conclusion was further supported by the HMBC correlation from H-3″ to an acetyl carbonyl carbon (δ_C170.5). Similarly, the difference between **4** and **2** was also determined to be the acetylation location. As evidenced by the chemical shifts for H-4′ (δ_H 4.91) and H-6′

(δ_H 3.69, 3.61) of **4** in comparison with other analogues, the 6′-*O*-acetyl group in **2** moved to C-4′ position in **4**, and the 2″,4″-*O*-diacetyl units retained. The aforementioned structural assignments for **3** and **4** were subsequently verified by careful check of 2D NNR spectra (Figs. S21-S32, SI). The structures of compounds **3** and **4** were hence elucidated.

Analyses of the (+)-HRESIMS data for **5** (inunicoside E) and **6** (inunicoside F) revealed ammonium adduct ion peaks at *m/z* 842.4177 and 842.4161 (both calcd 842.4169), respectively, which in combination with their ^{13}C NMR data assigned the same molecular formula of $C_{41}H_{60}O_{17}$ as **2**. As with the cases of **3**–**4**, compounds **5** and **6** were also regio-isomers of **2** with different acetyl substitution patterns. Inspection of the NMR data (Tables 1 and 2) uncovered that the major difference between **5** and **4** occurred to the disaccharide moiety, where H-3″ and H-4″ of **5** were observed at δ_H 4.87 and 4.01, respectively, while their counterparts of **4** appeared at δ_H 3.80 and 5.01, respectively. These observations suggested that the 4″-*O*-acetyl substitution in **4** was replaced by the 3″-*O*-acetyl substitution in **5**. Similarly, the difference between **6** and **4** was established that the 4″-*O*-acetyl group in **4** moved to C-6′ position in **6**, as supported by the chemical shift variations between the corresponding proton pairs of H-4″ (δ_H 5.01 for **4** Vs. 3.85 for **6**) and H_2-6′ (δ_H 3.69 & 3.61 for **4** Vs. 4.19 & 4.15 for **6**). Moreover, the structural assignments for **5** and **6** were also confirmed by detailed examination of 2D NMR data (Figs. S38–S49, SI).

(+)-HRESIMS analyses of compounds **7** (inunicoside G) and **8** (inunicoside H) exhibited ammonium and sodium adduct ion peaks at *m/z* 884.4279 (calcd 884.4274) 889.3827 and (calcd 889.3828), respectively, which were consistent with the same molecular formula of $C_{43}H_{62}O_{18}$ and suggested a pairs of isomers with an additional acetyl unit more than their cometabolites **2**–**6**. Analysis of the NMR data (Tables 2 and 3) for **7** confirmed this hypothesis, with diagnostic signals for four acetoxy groups at δ_H 2.13, 2.05, 2.04 and 2.00 (all s, 3H), as well as δ_C 171.1, 170.5, 170.4 and 169.8 (only carbonyl noted). Careful comparison between the NMR data for **7** and **2** indicated that the 3″-OH of **7** was further acetylated as evidenced by the chemical shifts for H-3″ (δ_H 4.97 for **7** Vs. 3.77 for **2**) of the two analogues, which was also

corroborated by the HMBC correlation from H-3″ to the newly introduced acetyl carbonyl carbon in **7**. Similar to the case of **2** and **4**, the difference between **8** and **7** was also attributed to that the acetylation pattern at 4′-OH and 6′-OH in the two analogues was reversed, which was clearly revealed by the chemical shift changes between the two proton pairs of H-4′ (δ_H 4.90 for **8** Vs. 3.54 for **7**) and H_2-6′ (δ_H 3.69 & 3.62 for **8** Vs. 4.45 & 4.23 for **7**). Compounds **7** and **8** were thus characterized as two penta-acylated diterpenoid glycosides with four acetyl and one isovaleryl groups all located on the sugar part, which was further confirmed by cautious inspections of 2D NMR spectroscopic data (Figs. S55–S66, SI).

Compounds **9** and **10** (inunicosides I and J) possessed the same molecular formula of $C_{43}H_{62}O_{18}$ as determined by their respective (+)-HRESIMS ammonium adduct ion peaks at *m/z* 884.4271 and 884.4280 (calcd 884.4274), as well as the ^{13}C NMR data. Detailed analyses of their NMR data (Tables 2 and 3) established that they were isomeric with **7** and **8**, and the structural differences were also assignable to the acetylation pattern on the disaccharide moeity. As with the case of **2** and **3**, compounds **9** and **10** only differed from each other in that the acetylation mode at 3″-OH and 4″-OH was inverted in their structures, and this was unambiguously demonstrated by the chemical shift variations between the two proton pairs of H-3″ (δ_H 3.78 for **9** Vs. 4.85 for **10**) and H-4″ (δ_H 5.00 for **9** Vs. 4.00 for **10**). Therefore, the two cometabolites had the same acylation pattern at all other positions except that **9** was 4″-*O*-acetylated and **10** was 3″-*O*-acetylated. Furhter examination of the full 2D NMR spectra (Figs. S72–S84, SI) of **9** and **10** corroborated their strucural assignments as shown.

Compound **11** (inunicoside K) was assigned a molecular formula of $C_{46}H_{64}O_{21}$, as deduced from the ammonium adduct ion peak at *m/z* 970.4284 $[M + NH_4]^+$ (calcd 970.4278) in the (+)-HRESIMS spectrum and the ^{13}C NMR data. Analysis of the NMR data (Tables 2 and 3) for **11** revealed that it was also a structural analogue of compounds **1**–**10** with the differences being depicted below. Twenty carbon resonances were observed for the aglycone moeity of **11**, which indicated an intact diterpenoid skeleton. Compared with **10**, the absence of the CH-4 methine signals (δ_H

2.69 and δ_C 43.5 for **10**), along with the appearance of a sp^3 quaternary carbon (δ_C 59.4, C-4) and a carboxyl carbonyl (δ_C 176.0, C-18) resonances, suggested that Me-18 in **11** was also oxidized to a carboxyl functionality [11], which was further confirmed by examination of 2D ^1H–^1H COSY and HMBC correlations (Fig. 4). As for the disaccharide fragment, all hydroxyls were acylated with an isovaleryloxy group at C-2′ and five acetoxy groups at C-4′, C-6′, C-2″ C-3″ and C-4″, respectively, as also supporpted by the HMBC correlations from these oxymethine protons to the corresponding ester carbonyl carbons. Careful comparisons of the remaining NMR data for **10** and **11**, including key proton-proton couplings, supported common structural features and identical relative configurations at all respective chiral centers between the two cometabolites, which was then corroborated by interpretation of 2D NMR data (Fig. 4). The structure of **11** was thereby characterized as shown, bearing an interesting 4-geminal carboxyl motiff and full acylation of the sugar part. Based on a biogenetic consideration and the highly consistent ECD curves of **2**–**11** (Fig. S99, SI) with that of **1**, the absolute configurations of **2**–**11** were also determined to be the same as that of **1**.

Compounds **1**–**12** were subjected to a series of bioassays (see experimental section). The assay results showed that only compound **11** exhibited moderate antibacterial activity against *S. aureus* ATCC 25923, with an IC_{50} value of 29.6 ± 3.5 μM, while others were inactive in all tested models.

3. Conclusion

Plants of the genus *Inula* grow throughout Europe, Africa and Asia, and many species are used as folk medicines by local residents [6]. This genus is very famous in the literature for its rich sesquiterpenoid constituents and their diverse biological properties especially anti-tumor and anti-inflammatory activities [6], whereas studies on the diterpenoid ingredients remain very limited. On reviewing the literature, in addition to the several diterpene quinones isolated from *I. royleana* in 1962 [15] and 1975 [16], the *ent*-kaurane diterpenoids from Chinese *Inula* species in later work [9,17] all bear at least one carboxyl group and/or sugar moiety. Therefore, the

previously focused attention on sesquiterpenes and the separation difficulty due to increased polarity of diterpenes could account for the limited diterpenoid reports on *Inula* plants. As we know, triterpenoid saponins are widely distributed in many plant species, while the diterpenoid glycosides present a much less occurrence in nature, so the isolation of this array of *ent*-kaurane diterpenoid glycosides from *I. japonica* is very interesting and increases the structural diversity of this class of natural products. Moreover, the diverse acylation patterns of these glycosides indicate the presence of some specific acylation enzymes in this species, which definitely deserves further investigations from researchers of related areas.

4. Experimental

4.1. General experimental procedures

Optical rotations were measured on a Rudolph VI polarimeter (Rudolph Research Analytical, Hackettstown, USA) with a 10 cm length cell. UV and ECD spectra were obtained on a Chirascan Spectrometer (Applied Photophysics Ltd., Leatherhead, UK) with a 1 mm pathway cell. NMR experiments were performed on a Bruker Avance DRX600 spectrometer (Bruker BioSpin AG, Fällanden, Switzerland) and referenced to residual solvent peaks (δ_C 49.00 and δ_H 3.31 ppm for CD_3OD; δ_C 77.16 and δ_H 7.26 ppm for $CDCl_3$). ESIMS analyses were carried out on an Agilent 1260-6460 Triple Quad LC-MS instrument (Agilent Technologies Inc., Waldbronn, Germany). HR-ESIMS data were acquired on an Agilent 6545 QTOF mass spectrometer (Agilent Technologies Inc., Waldbronn, Germany). All HPLC analyses and separations were performed on an Agilent 1260 series LC instrument (Agilent Technologies Inc., Waldbronn, Germany). D101-macroporous absorption resin (Sinopharm Chemical Reagent Co. Ltd., Shanghai, China), CHP20/P120 MCI gel (75–150 μm, Mitsubishi Chemical Co., Tokyo, Japan) and silica gel (300–400 mesh, Qingdao Marine Chemical Co. Ltd., Qingdao, China) were used for column chromatography (CC). Agilent ZORBAX SB-C_{18} columns (5 μm, 4.6 × 250 and 9.4 × 250 mm; Agilent Technologies Inc., Santa Clara, USA) were used for HPLC analyses and separations. All solvents used for CC were of analytical grade (Tianjin Fuyu Fine Chemical Co.

Ltd., Tianjin, China) and solvents used for HPLC were of HPLC grade (Oceanpak Alexative Chemical Ltd., Goteborg, Sweden). All solvent mixtures used for analyses and separations (HPLC & CC) were presented in the ratio of volume to volume, unless otherwise specified.

4.2. Plant material

The flowers of *Inula japonica* Thunb. were collected in September 2016 in Mount Kunyu of Shandong Province, China, and were authenticated by Prof. Guo-hua Ye from Shandong College of Traditional Chinese Medicine. A voucher specimen has been deposited at School of Biological Science and Technology, University of Jinan (Accession number: npmc-003).

4.3. Extraction and isolation

The air-dried flowers of *I. japonica* (15 kg) were extracted with 95% EtOH at room temperature for four times (one week per time) to afford a crude extract (1.5 kg). The extract was suspended in 3.0 L water and then partitioned successively with EtOAc (3 × 2.0 L) and *n*-BuOH (3 × 2.0 L) to afford the corresponding layers. After evaporation of solvents under reduced pressure, the EtOAc (750 g) and *n*-BuOH (120 g) soluble parts were finally obtained.

The EtOAc partition was subjected to CC over D101 macroporous absorption resin, eluted with EtOH-H_2O (50%, 80% and 95%) to get three fractions. The 80% ethanol elution was separated by MCI gel CC (MeOH-H_2O, 50%, 80% and 100%) to afford three fractions (A, B and C). Fraction A (50%, 60 g) was chromatographed on a silica gel column (petroleum ether (PE)-acetone, 20:1 to 1:2) to give five subfractions (A1–A5), and fraction A5 was separated by silica gel CC (PE-EtOAc, 5:1 to 1:2) to give four subfractions (A5-1–A5-4). Fraction A5-1 (0.3 g) was subjected to passage over a silica gel column, eluted with $CHCl_3$-MeOH (100:1 to 30:1), to give three subfractions, and the third one was then purified by semi-preparative HPLC (60% MeCN-H_2O) to afford compound **7** (6.8 mg, t_R = 14.1 min). Using similar procedures, fraction A5-3 (3.1 g) was separated into three subfractions (A5-3a–A5-3c), and each of them was successively purified by semi-preparative HPLC (48% MeCN-H_2O) to

yield compounds **2**/**9**/**10** (17.8/26.7/18.4 mg; t_R = 16.1/22.3/27.1 min), **3** (17.2 mg, t_R = 18.2 min) and **8** (11.7 mg, t_R = 20.0 min), respectively. Fraction A5-4 (3.6 g) was fractionated by silica gel CC first with $CHCl_3$-MeOH (100:1 to 30:1) and then with PE-EtOAc (3:1 to 1:2), and the major elution containing the target compounds were finally purified by semi-preparative HPLC (40% MeCN-H_2O) to afford **1** (13.8 mg, t_R = 12.7 min), **4** (6.3 mg, t_R = 19.5 min), **6** (20.2 mg, t_R = 20.8 min), **5** (24.1 mg, t_R = 24.7 min) and **11** (9.4 mg, t_R = 36.4 min).

The *n*-BuOH partition was chromatographed on a silica gel column (CH_2Cl_2-MeOH-H_2O, 130:13:10) to furnish four subfractions (D1–D4). Fraction D3 was separated by silica gel CC (EtOAc-MeOH-H_2O, 5:1:1) to give one major portion which was further purified by semi-preparative HPLC (16% MeCN-H_2O) to furnish compound **12** (74.3 mg, t_R = 30.1 min).

*Inunicoside A (**1**)*: white amorphous powder; $[\alpha]_D^{25}$ –39.1 (*c* 1.36, MeOH); ECD (*c* 0.73, MeOH) λ ($\Delta\varepsilon$) 206 (5.63); ^{1}H and ^{13}C NMR data ($CDCl_3$), see Tables 1 and 2; (+)-ESIMS: *m/z* 805.3 $[M + Na]^+$; (–)-ESIMS: *m/z* 817.3 $[M + Cl]^-$; (+)-HRESIMS: *m/z* 805.3607 $[M + Na]^+$ (calcd for $C_{39}H_{58}O_{16}Na$, 805.3617).

*Inunicoside B (**2**)*: white amorphous powder; $[\alpha]_D^{25}$ –27.6 (*c* 1.77, MeOH); ECD (*c* 0.73, MeOH) λ ($\Delta\varepsilon$) 206 (6.37); ^{1}H and ^{13}C NMR data ($CDCl_3$), see Tables 1 and 2; (+)-ESIMS: *m/z* 842.3 $[M + NH_4]^+$; (–)-ESIMS: *m/z* 823.2 $[M - H]^-$, 859.3 $[M + Cl]^-$; (+)-HRESIMS: *m/z* 842.4188 $[M + NH_4]^+$ (calcd for $C_{41}H_{64}NO_{17}$, 842.4169).

*Inunicoside C (**3**)*: white amorphous powder; $[\alpha]_D^{25}$ –36.7 (*c* 1.70, MeOH); ECD (*c* 0.73, MeOH) λ ($\Delta\varepsilon$) 206 (6.64); ^{1}H and ^{13}C NMR data ($CDCl_3$), see Tables 1 and 2; (–)-ESIMS: *m/z* 859.1 $[M + Cl]^-$; (+)-HRESIMS: *m/z* 842.4193 $[M + NH_4]^+$ (calcd for $C_{41}H_{64}NO_{17}$, 842.4169).

*Inunicoside D (**4**)*: white amorphous powder; $[\alpha]_D^{25}$ –30.4 (*c* 0.62, MeOH); ECD (*c* 0.73, MeOH) λ ($\Delta\varepsilon$) 206 (7.11); ^{1}H and ^{13}C NMR data ($CDCl_3$), see Tables 1 and 2; (+)-ESIMS: *m/z* 842.3 $[M + NH_4]^+$; (–)-ESIMS: *m/z* 823.2 $[M - H]^-$, 859.3 $[M + Cl]^-$; (+)-HRESIMS: *m/z* 842.4183 $[M + NH_4]^+$ (calcd for $C_{41}H_{64}NO_{17}$, 842.4169).

*Inunicoside E (**5**)*: white amorphous powder; $[\alpha]_D^{25}$ –37.9 (*c* 2.41, MeOH); ECD (*c*

0.73, MeOH) λ ($\Delta\varepsilon$) 206 (6.49); ^{1}H and ^{13}C NMR data ($CDCl_3$), see Tables 1 and 2; (–)-ESIMS: *m/z* 823.3 $[M - H]^-$, 859.3 $[M + Cl]^-$; (+)-HRESIMS: *m/z* 842.4177 $[M + NH_4]^+$ (calcd for $C_{41}H_{64}NO_{17}$, 842.4169).

*Inunicoside F (**6**)*: white amorphous powder; $[\alpha]_D^{25}$ −73.6 (*c* 2.00, MeOH); ECD (*c* 0.73, MeOH) λ ($\Delta\varepsilon$) 206 (6.50); ^{1}H and ^{13}C NMR data ($CDCl_3$), see Tables 1 and 2; (+)-ESIMS: *m/z* 842.3 $[M + NH_4]^+$; (–)-ESIMS: *m/z* 823.3 $[M - H]^-$; (+)-HRESIMS: *m/z* 842.4161 $[M + NH_4]^+$ (calcd for $C_{41}H_{64}NO_{17}$, 842.4169).

*Inunicoside G (**7**)*: white amorphous powder; $[\alpha]_D^{25}$ −41.2 (*c* 0.65 MeOH); ECD (*c* 0.80, MeOH) λ ($\Delta\varepsilon$) 206 (6.23); ^{1}H and ^{13}C NMR data ($CDCl_3$), see Tables 2 and 3; (–)-ESIMS: *m/z* 865.5 $[M - H]^-$, 901.5 $[M + Cl]^-$; (+)-HRESIMS: *m/z* 884.4279 $[M + NH_4]^+$ (calcd for $C_{43}H_{66}NO_{18}$, 884.4274).

*Inunicoside H (**8**)*: white amorphous powder; $[\alpha]_D^{25}$ −45.6 (*c* 1.17, MeOH); ECD (*c* 0.80, MeOH) λ ($\Delta\varepsilon$) 206 (6.43); ^{1}H and ^{13}C NMR data ($CDCl_3$), see Tables 2 and 3; (+)-ESIMS: *m/z* 889.1 $[M + Na]^+$; (–)-ESIMS: *m/z* 865.4 $[M - H]^-$, 901.3 $[M + Cl]^-$; (+)-HRESIMS: *m/z* 889.3827 $[M + Na]^+$ (calcd for $C_{43}H_{62}O_{18}Na$, 889.3828).

*Inunicoside I (**9**)*: white amorphous powder; $[\alpha]_D^{25}$ −31.7 (*c* 2.66, MeOH); ECD (*c* 0.80, MeOH) λ ($\Delta\varepsilon$) 206 (6.65); ^{1}H and ^{13}C NMR data ($CDCl_3$), see Tables 2 and 3; (+)-ESIMS: *m/z* 884.3 $[M + NH_4]^+$; (–)-ESIMS: *m/z* 865.3 $[M - H]^-$, 901.2 $[M + Cl]^-$; (+)-HRESIMS: *m/z* 884.4271 $[M + NH_4]^+$ (calcd for $C_{43}H_{66}NO_{18}$, 884.4274).

*Inunicoside J (**10**)*: white amorphous powder; $[\alpha]_D^{25}$ −24.3 (*c* 1.83, MeOH); ECD (*c* 0.80, MeOH) λ ($\Delta\varepsilon$) 206 (6.88); ^{1}H and ^{13}C NMR data ($CDCl_3$), see Tables 2 and 3; (+)-ESIMS: *m/z* 884.3 $[M + NH_4]^+$; (+)-HRESIMS: *m/z* 884.4280 $[M + NH_4]^+$ (calcd for $C_{43}H_{66}NO_{18}$, 884.4274).

*Inunicoside K (**11**)*: white amorphous powder; $[\alpha]_D^{25}$ −38.4 (*c* 1.24, MeOH); ECD (*c* 0.85, MeOH) λ ($\Delta\varepsilon$) 205 (6.67); ^{1}H and ^{13}C NMR data (CD_3OD), see Tables 2 and 3; (–)-ESIMS: *m/z* 951.3 $[M - H]^-$; (+)-HRESIMS: *m/z* 970.4284 $[M + NH_4]^+$ (calcd for $C_{46}H_{68}NO_{21}$, 970.4278).

4.4. Determination of D-glucose and L-arabinose

A solution of *ca.* 1.0 mg **1** in 2.0 N HCl (3.0 mL) was stirred at 90 °C for 4 h. After removal of excess HCl under reduced pressure, the residual aqueous mixture was filtered to remove the aglycone part and then evaporated under reduced pressure to afford the free monosaccharide. The monosaccharide was dissolved in ethanol and then excess (*S*)-(−)-1-phenylethylamine and $NaBH_3CN$ were added. With a catalytic amount of acetic acid added, the mixture was stirred at 40 °C for 3 h. After evaporation of the solvent, the residue was stirred with acetic anhydride in pyridine at room temperature for 5 h to obtain the amino derivative. Using the same method, the amino derivatives of authentic D- and L-glucoses, D- and L-arabinoses were obtained. These derivatives were subjected to HPLC analysis on an Agilent ZORBAX SB-C_{18} column (5 μm, 4.6 × 250 mm) with 52% MeCN-H_2O as mobile phase at 1.00 mL/min. As shown in Fig. S95 (SI), the retention times of standard D- and L-glucoses, D- and L-arabinoses were observed at t_R 7.158, 6.819, 6.053 and 5.953 min, respectively. The retention times of the hydrolytic samples of **1** were observed at t_R 7.174 and 5.967 min, respectively, and thus the D-glucose and L-arabinose were determined for **1**.

*4.5. Enzymatic hydrolysis of **1***

Compound **1** (6.0 mg) and snailase (1.2 mg) were mixed in 2.0 mL sodium acetate buffer solution (pH 5.0) and then stirred at 37 °C overnight. After the hydrolysis, 2.0 mL $CHCl_3$ was added to the aforementioned buffer solution, mixed completely and then layered. When solvents of this $CHCl_3$ extract were evaporated under reduced pressure, the aglycone (**1a**) was then obtained by purification on semi-preparative HPLC (44% MeCN-H_2O, 3.00 mL/min), with t_R at 6.8 min. Atractyligenin (**1a**): white amorphous powder; $[\alpha]_D^{25}$ −131.2 (*c* 0.22, MeOH); ECD (*c* 0.31, MeOH) λ (Δε) 206 (4.26); ^1H and ^{13}C NMR data (CD_3OD), see Table S4 in SI; (−)-ESIMS: *m*/*z* 319.1 $[M - H]^-$, 355.1 $[M + Cl]^-$.

4.6. ECD calculations

The ChemDraw_Pro_14.1 software with MM2 force field was used to establish the initial conformations of target molecules. Conformational searches using mixed torsional/Low-mode sampling method with MMFFs force field in an energy window

of 3.01 kcal/mol were carried out by means of the conformational search module in the Maestro 10.2 software [18]. The re-optimization and the following TD-DFT calculations of the re-optimized conformations were all performed with Gaussian 09 software at the B3LYP/6-311G(d,p) level *in vacuo* for **1** and **1a**. Frequency analysis was performed as well to confirm that the re-optimized conformers were at the energy minima. Finally, the SpecDis 1.64 software [19] was used to obtain the Boltzmann-averaged ECD spectra.

4.7 Bioassays

4.7.1 Cytotoxic assay

The cytotoxicity toward two human female cancer cell lines, MDA-MB-231 (breast) and Hela (cervical), was screened by the MTT method as reported formerly [20]. A single concentration of 30 μM was chosen for the primary screening. Adriamycin was used as the positive control with IC_{50} values of 0.67 ± 0.04 and 0.91 ± 0.11 μM for MDA-MB-231 and HeLa cells, respectively.

4.7.2 NO production inhibitory assay

The inhibitory activity against LPS-induced NO production in murine RAW264.7 macrophages was performed by colorimetric assay based on the Griess reaction, as previously described [21]. The initial screening concentration was set as 50 μM (Table S2, SI). Dexamethasone was used as a positive control (IC_{50} = 15.3 ± 1.7 μM).

4.7.3 Anti-acetylcholinesterase assay

The AChE inhibitory activity was tested using modified Ellman′s method as we described previously [22]. The preliminary screening concentration was set as 50 μM (Table S3, SI). Galantamin was used as a positive control (IC_{50} = 0.85 ± 0.12 μM).

4.7.4 α-Glucosidase inhibitory assay

The *α*-glucosidase inhibitory activity was examined by a previously described method in our recent article [23]. All the isolates were first tested at a primary concentration of 100 μM. Acarbose was as used as a control drug (IC_{50} = 883 ± 189 μM).

4.7.5 Antibacterial assay

The antibacterial activity against two Gram-positive trains, *Staphylococcus aureus* ATCC 25923 and *Bacillus subtilis* ATCC 6633, was tested using liquid growth inhibition method as we described previously [24]. The initial testing concentration was set at 50 μM, and only compounds with >50% growth inhibition rate were further subjected for IC_{50} measurements. Penicillin was used as the positive control (IC_{50} = 0.12 ± 0.03 and 0.23 ± 0.02 μM for *S. aureus* and *B. subtilis*, respectively).

4.7.6 Pancreatic lipase inhibitory assay

Pancreatic lipase inhibitory activity was evaluated referring to the procedures as described in the literature [25]. All the compounds was screened at the initial concentration of 50 μM. Orlistat was used as a positive control (IC_{50} = 0.84 ± 0.32 μM).

Conflict of interest

The authors declare no conflicts of interest.

Acknowledgements

This project was financially supported by Natural Science Foundation of Shandong Province [No. JQ201721], the Young Taishan Scholars Program [No. tsqn20161037], and Shandong Talents Team Cultivation Plan of University Preponderant Discipline [No. 10027]. We also thank Prof. Guo-hua Ye from Shandong College of Traditional Chinese Medicine for the identification of the plant material.

Appendix A. Supplementary data

Supplementary data to this article can be found online at https://xxx

References

[1] Flora of China Editorial Committee of Chinese Academy of Sciences, The Flora of China, Vol. 75, Science Press, Beijing, 1999, p. 263.

[2] National Pharmacopoeia Committee, in: Pharmacopoeia of the People's Republic of China, Part 1, China Medical Science and Technology Press,

Beijing, 2015, p. 325.

[3] Q.H. Jin, J.W. Lee, H. Jang, J.E. Choi, D.H. Lee, J.T. Hong, Y.S. Kim, M.K. Lee, B.Y. Hwang, J. Nat. Prod. 79 (2016) 1548−1553.

[4] Y. Li, Z.Y. Ni, M.C. Zhu, M. Dong, S.M. Wang, Q.W. Shi, M.L. Zhang, Y.F. Wang, C.H. Huo, H. Kiyota, B. Cong, Z NATURFORSCH C. 67 (2012) 375−380.

[5] J.J. Qin, L.Y. Wang, J.X. Zhu, H.Z. Jin, J.J. Fu, X.F. Liu, H.L. Li, W.D. Zhang, Chem. Commun. 47 (2011) 1222−1224.

[6] G.W. Wang, J.J. Qin, X.R. Cheng, Y.H. Shen, L. Shan, H.Z. Jin, W.D. Zhang, Expert Opin. Invest. Drugs 23 (2014) 317−345.

[7] X.D. Wu, L.F. Ding, W.C. Tu, H. Yang, J. Su, L.Y. Peng, Y. Li, Q.S. Zhao, Phytochemistry 129 (2016) 68−76.

[8] J.J. Qin, H.Z. Jin, J.X. Zhu, J.J. Fu, Q. Zeng, X.R. Cheng, Y. Zhu, L. Shan, S.D. Zhang, Y.X. Pan, W.D. Zhang, Tetrahedron 66 (2010) 9379−9388.

[9] J.J. Qin, J.X. Zhu, W.D. Zhang, Y. Zhu, J.J. Fu, X.H. Liu, H.Z. Jin, Arch. Pharm. Res. 32 (2009) 1369−72.

[10] Z.P. Yu, J.S. Zhang, Q.Q. Zhang, S.J. Yu, Y.Y. Zhang, J.H. Yu, H. Zhang, Fitoterapia (2019). https://doi.org/10.1016/j.fitote.2019.104292

[11] R. Lang, T. Fromme, A. Beusch, A. Wahl, M. Klingenspor, T. Hofmann, Phytochemistry (Elsevier) 93 (2013) 124−135.

[12] S.Y. Lee, W.S. Suh, H.K. Kim, I.K. Lee, S.U. Choi, K.H. Kim, K.R. Lee, Heterocycles 91 (2015) 1187-1197.

[13] Z.P. Yu, Y.Y. Wang, S.J. Yu, J. Bao, J.H. Yu, H. Zhang, Fitoterapia 135 (2019) 99-106.

[14] F. Brucoli, M.T. Borrello, P. Stapleton, G.N. Parkinson, S. Gibbons, J. Nat. Prod. 75 (2012) 1070−1075.

[15] O.E. Edwards, G. Feniak, M. Los, Can. J. Chem. 40 (1962) 1540−1546.

[16] S.V. Bhat, P.S. Kalyanaraman, H. Kohl, N.J. De Souza, Tetrahedron 31 (1975) 1001−1004.

[17] Y. Shao, N.S. Bai, B.N. Zhou, Phytochemistry 42 (1996) 783−786.

[18] M.J. Frisch, G.W. Trucks, H.B. Schlegel, G.E. Scuseria, M.A. Robb, J.R. Cheeseman, G. Scalmani, V. Barone, B. Mennucci, G.A. Petersson, H. Nakatsuji, M. Caricato, X. Li, H.P. Hratchian, A.F. Izmaylov, J. Bloino, G. Zheng, J.L. Sonnenberg, M. Hada, M. Ehara, K. Toyota, R. Fukuda, J. Hasegawa, M. Ishida, T. Nakajima, Y. Honda, O. Kitao, H. Nakai, T. Vreven, J.A. Montgomery, Jr., J.E. Peralta, F. Ogliaro, M. Bearpark, J.J. Heyd, E. Brothers, K.N. Kudin, V.N. Staroverov, R. Kobayashi, J. Normand, K. Raghavachari, A. Rendell, J.C. Burant, S.S. Iyengar, J. Tomasi, M. Cossi, N. Rega, J.M. Millam, M. Klene, J.E. Knox, J.B. Cross, V. Bakken, C. Adamo, J. Jaramillo, R. Gomperts, R.E. Stratmann, O. Yazyev, A.J. Austin, R. Cammi, C. Pomelli, J.W. Ochterski, R.L. Martin, K. Morokuma, V.G. Zakrzewski, G.A. Voth, P. Salvador, J.J. Dannenberg, S. Dapprich, A.D. Daniels, O. Farkas, J.B. Foresman, J.V. Ortiz, J. Cioslowski, and D.J. Fox, Gaussian 09 Revision B.01, Gaussian Inc, Wallingford CT, 2009.

[19] T. Bruhn, A. Schaumloeffel, Y. Hemberger, G. Bringmann, Chirality 25 (2013) 243–249.

[20] M. He, L. Jiang, B. Li, G. Wang, J. Wang, Y. Fu, Oncotarget 8 (2017) 65100–65110.

[21] J.J. Zhao, Y.Q. Guo, D.P. Yang, X. Xue, Q. Liu, L.P. Zhu, S. Yin, Z.M. Zhao, J. Nat. Prod. 79 (2016) 2257–2263.

[22] Z.Q. Cheng, K.K. Zhu, J. Zhang, J.L. Song, L.A. Muehlmann, C.S. Jiang, C.L. Liu, H. Zhang, Bioorg. Chem. 83 (2019) 277–288.

[23] J. Sun, J.H. Yu, J.S. Zhang, X.Q. Song, J. Bao, H. Zhang, Chem. Biodiversity 16 (2019). https://doi.org/10.1002/cbdv.201800581.

[24] J. Bao, H.J. Zhai, K.K. Zhu, J.H. Yu, Y.Y. Zhang, Y.Y. Wang, C.S. Jiang, X. Zhang, Y. Zhang, H. Zhang, Mar. Drugs 16 (2018). https://doi.org/10.3390/md16050174.

[25] X.C. Jia, D. Yang, H.H. Xie, Y.M. Jiang, X.Y. Wei, J. Funct. Foods 32 (2017) 419–425.

Table 1. ^{1}H NMR spectroscopic data of compounds 1–6 in $CDCl_3$.

No	1	2	3	4	5	6
1α	2.19, brdd (12.2, 5.0)	2.29, brdd (13.0, 5.2)	2.27, brdd (12.5, 4.9)	2.22, m	2.21, m	2.27, m
1β	0.76, dd (12.2, 12.0)	0.79, dd (13.0, 10.8)	0.79, dd (12.5, 11.5)	0.79, t (12.1)	0.77, t (12.1)	0.81, t (12.1)
2	4.23, m	4.12, m	4.12, m	4.24, m	4.24, m	4.13, m
3α	2.42, dt (12.0, 2.7)	2.33, dt (12.4, 2.6)	2.33, m	2.41, m	2.41, dt (12.0, 2.7)	2.35, dt (12.1, 2.5)
3β	1.18, td (12.0, 5.3)	1.22, td (12.4, 4.9)	1.21, td (12.0, 5.4)	1.20, m	1.17, td (12.0, 5.2)	1.23, td (12.1, 5.4)
4	2.68, m	2.68, m	2.68, m	2.70, m	2.69, m	2.70, m
5	1.44, m	1.45, m	1.43, m	1.45, m	1.43, m	1.45, m
6α	1.91, m	1.88, m	1.88, m	1.91, m	1.90, m	1.88, m
6β	1.64, m	1.64, m	1.63, m	1.65, m	1.64, m	1.65, m
7α	1.73, dt (13.4, 3.2)	1.73, dt (13.2, 3.1)	1.72, dt (13.2, 2.9)	1.74, dt (13.5, 3.1)	1.73, dt (13.4, 3.2)	1.74, dt (13.4, 3.3)
7β	1.43, m	1.43, m	1.42, m	1.44, m	1.43, m	1.44, m
9	1.03, brd (8.1)	1.03, brd (8.0)	1.03, brd (8.0)	1.04, brd (8.0)	1.02, brd (8.1)	1.04, brd (8.1)
11α	1.54, m	1.56, m	1.58, m	1.54, m	1.54, m	1.56, m
11β	1.41, m	1.41, m	1.40, m	1.43, m	1.42, m	1.43, m
12α	1.57, m	1.57, m	1.55, m	1.56, m	1.56, m	1.56, m
12β	1.48, m	1.47, m	1.48, m	1.48, m	1.47, m	1.47, m
13	2.74, m	2.73, m	2.73, m	2.75, m	2.74, m	2.74, m
14α	1.86, brd (11.8)	1.83, brd (11.7)	1.83, brd (11.5)	1.85, brd (11.8)	1.85, brd (11.7)	1.84, brd (11.5)
14β	1.39, dd (11.8, 5.0)	1.38, dd (11.7, 5.0)	1.38, dd (11.5, 4.9)	1.39, dd (11.8, 5.2)	1.39, dd (11.7, 5.3)	1.39, dd (11.5, 4.9)
15	3.80, s	3.80, s	3.80, s	3.81, s	3.81, s	3.81, s
17a	5.21, brs	5.21, brs	5.21, brs	5.21, brs	5.21, brs	5.21, brs
17b	5.08, brs	5.08, brs	5.07, brs	5.08, brs	5.08, brs	5.08, brs
20	0.97, s	0.96, s	0.96, s	0.97, s	0.96, s	0.96, s
1′	4.60, d (8.0)	4.51, d (8.0)	4.50, d (8.1)	4.60, d (8.0)	4.59, d (8.0)	4.55, d (8.0)
2′	4.94, dd (9.1, 8.0)	4.90, dd (9.4, 8.0)	4.89, dd (9.3, 8.1)	4.99, dd (9.2, 8.0)	4.95, dd (9.4, 8.0)	4.97, dd (9.3, 8.0)
3′	3.64, dd (9.2, 9.1)	3.59, dd (9.4, 9.2)	3.62, dd (9.3, 8.8)	3.87, dd (9.3, 9.2)	3.84, dd (9.4, 9.1)	3.83, dd (9.3, 8.8)
4′	3.56, dd (9.2, 9.2)	3.52, dd (9.6, 9.2)	3.51, m	4.91, dd (9.7, 9.3)	4.91, dd (9.6, 9.1)	4.98, dd (8.8, 8.4)
5′	3.42, m	3.51, m	3.51, m	3.51, m	3.51, m	3.67, m
6′a	3.93, dd (11.9, 3.1)	4.44, dd (11.9, 1.8)	4.45, dd (12.0, 2.3)	3.69, dd (12.5, 2.3)	3.69, dd (12.4, 2.1)	4.19, dd (12.2, 5.2)
6′b	3.76, dd (11.9, 5.7)	4.24, dd (11.9, 5.0)	4.22, dd (12.0, 6.2)	3.61, dd (12.5, 5.8)	3.61, dd (12.4, 5.1)	4.15, dd (12.2, 2.5)
1″	4.46, d (6.6)	4.41, d (7.1)	4.43, d (7.2)	4.53, d (5.2)	4.47, d (5.3)	4.51, d (5.2)
2″	4.95, dd (7.6, 6.6)	4.96, dd (9.3, 7.1)	5.19, dd (9.6, 7.2)	4.79, dd (7.6, 5.2)	4.99, dd (7.6, 5.3)	4.76, dd (6.4, 5.2)
3″	3.80, dd (7.6, 3.9)	3.77, dd (9.3, 3.7)	4.89, dd (9.6, 3.3)	3.80, dd (7.6, 3.3)	4.87, dd (7.6, 3.5)	3.69, dd (6.4, 3.8)
4″	5.06, m	5.06, m	4.07, m	5.01, m	4.01, m	3.85, m
5″a	4.14, dd (13.0, 3.8)	4.11, dd (13.3, 2.9)	4.07, dd (13.7, 3.2)	3.98, dd (12.5, 5.6)	3.89, dd (12.0, 5.5)	3.79, dd (12.0,6.2)
5″b	3.60, dd (13.0, 2.1)	3.60, dd (13.3, 1.8)	3.62, dd (13.7, 2.2)	3.51, dd (12.5, 2.9)	3.51, dd (12.0, 2.7)	3.50, dd (12.0, 3.2)
2‴a	2.24, dd (14.9, 7.4)	2.24, dd (14.9, 7.1)	2.22, dd (15.1, 7.2)	2.26, dd (15.1, 7.1)	2.25, dd (15.1, 7.0)	2.27, dd (15.1, 7.0)
2‴b	2.21, dd (14.9, 7.1)	2.21, dd (14.9, 7.1)	2.20, dd (15.1, 7.0)	2.22, dd (15.1, 7.0)	2.21, dd (15.1, 7.0)	2.22, dd (15.1, 7.1)
3‴	2.11, m	2.11, m	2.10, m	2.11, m	2.10, m	2.12, m
4‴	0.99, d (6.7)	0.99, d (6.6)	0.99, d (6.6)	0.99, d (6.7)	0.98, d (6.6)	0.98, d (6.7)
5‴	0.98, d (6.6)	0.98, d (6.6)	0.98, d (6.6)	0.98, d (6.6)	0.97, d (6.6)	0.98, d (6.6)
4′-OAc				2.05, S	2.09, S	2.07, s
6′-OAc		2.05, s	2.05, s			2.05, s
2″-OAc	2.11, s	2.10, s	2.03, s	2.10, s	2.03, s	2.08, s
3″-OAc			2.09, s		2.09, s	
4″-OAc	2.15, s	2.15, s		2.13, s		

Table 2. ^{13}C NMR spectroscopic data of compounds 1–11.

No.	**1**[a]	**2**[a]	**3**[a]	**4**[a]	**5**[a]	**6**[a]	**7**[a]	**8**[a]	**9**[a]	**10**[a]	**11**[b]
1	47.3	47.5	47.4	47.2	47.2	47.4	47.5	47.2	47.4	47.4	48.5
2	71.3	73.3	73.2	71.7	71.4	71.8	73.3	71.6	73.3	73.3	74.0
3	34.2	34.2	34.2	33.9	33.9	34.2	34.2	33.8	34.3	34.1	41.1
4	43.5	43.6	43.6	43.4	43.5	43.5	43.6	43.5	43.6	43.5	59.4
5	49.3	49.1	49.1	49.3	49.3	49.1	49.1	49.3	49.1	49.0	52.2
6	25.4	25.4	25.4	25.4	25.4	25.4	25.4	25.4	25.4	25.4	24.1
7	34.9	34.9	34.9	34.9	34.9	34.9	34.9	34.9	34.9	34.8	36.2
8	47.8	47.7	47.7	47.8	47.7	47.7	47.7	47.7	47.7	47.7	48.9
9	52.7	52.6	52.7	52.7	52.7	52.6	52.6	52.7	52.7	52.6	54.9
10	40.8	40.7	40.7	40.8	40.8	40.7	40.7	40.8	40.7	40.7	41.4
11	18.3	18.3	18.3	18.3	18.3	18.3	18.3	18.3	18.3	18.3	19.3
12	32.6	32.6	32.6	32.5	32.5	32.6	32.6	32.5	32.6	32.5	33.6
13	42.4	42.3	42.34	42.4	42.4	42.3	42.3	42.3	42.4	42.3	43.6
14	36.4	36.4	36.4	36.4	36.4	36.4	36.4	36.4	36.4	36.4	37.3
15	82.8	82.7	82.7	82.8	82.8	82.7	82.7	82.8	82.7	82.7	83.4
16	160.0	159.9	159.9	160.0	160.0	159.9	159.9	160.0	160.0	159.8	160.2
17	108.9	108.9	108.9	108.9	108.9	109.0	108.9	108.9	108.9	108.9	109.1
18											176.0
19	179.3	180.2	180.1	179.2	179.3	180.0	180.4	179.5	179.5	180.0	175.9
20	16.9	16.8	16.8	16.9	16.8	16.8	16.8	16.8	16.8	16.7	17.7
1′	99.0	100.3	100.3	98.8	98.7	100.0	100.3	98.9	100.0	100.1	100.8
2′	72.2	72.3	72.3	72.8	72.7	72.7	72.3	72.8	72.7	72.7	74.2
3′	83.4	83.9	83.6	80.2	80.7	80.5	83.9	80.3	80.3	80.6	80.6
4′	69.4	68.9	69.1	69.6	69.7	69.3	68.8	69.7	69.3	69.2	70.0
5′	75.8	73.6	73.6	74.4	74.4	73.4	73.6	74.5	71.8	71.8	72.9
6′	62.8	63.6	63.7	62.0	61.9	62.7	63.6	62.0	62.7	62.7	63.4
1″	100.7	101.1	101.4	100.4	100.7	100.2	101.6	100.7	100.5	100.8	102.2
2″	72.0	72.1	67.0	72.1	69.3	72.1	68.7	69.2	72.2	69.4	70.6
3″	70.2	70.5	72.7	69.6	71.9	70.6	70.3	69.4	69.7	72.0	71.7
4″	70.2	70.5	66.8	69.5	65.7	66.4	67.7	66.9	69.6	65.7	69.3
5″	62.8	63.5	65.9	60.9	63.9	63.0	64.3	61.7	61.1	64.2	64.0
1‴	171.4	171.2	171.2	171.4	171.3	171.6	171.2	171.2	171.4	171.2	173.0
2‴	43.7	43.7	43.6	43.6	43.5	43.5	43.6	43.5	43.6	43.4	44.4
3‴	25.8	25.7	25.7	25.7	25.7	25.6	25.7	25.7	25.7	25.6	26.7
4‴	22.8	22.8	22.8	22.8	22.8	22.8	22.8	22.8	22.8	22.8	23.0
5‴	22.8	22.8	22.8	22.8	22.8	22.8	22.8	22.7	22.8	22.8	23.0
4′-OAc				21.0	21.2	21.2		21.1	21.0	21.2	20.6
				170.4	170.9	170.3		170.4	169.8	170.3	171.6
6′-OAc		21.1	21.0			21.0	20.8		21.0	21.0	21.1
		171.2	171.2			171.0	171.1		171.0	171.0	172.4
2″-OAc	21.0	20.9	20.8	21.1	20.9	21.0	21.1	20.9	21.0	20.8	20.7
	171.2	171.4	170.1	170.1	169.8	171.2	169.8	169.6	171.2	169.8	171.3
3″-OAc			21.1		21.1		20.7	20.8		21.1	20.7
			170.5		170.8		170.4	170.6		170.8	171.7
4″-OAc	21.2	21.2		21.2			21.1	21.1	21.2		20.7
	170.8	170.9		170.8			170.5	170.4	170.7		171.8

[a] Data were measured in $CDCl_3$. [b] Data were measured in methanol-d_4.

Table 3. ^{1}H NMR spectroscopic data of compounds 7–11.

No.	**7**[a]	**8**[a]	**9**[a]	**10**[a]	**11**[b]
1α	2.29, m	2.21, m	2.28, m	2.28, m	2.30, m
1β	0.79, t (12.1)	0.78, t (12.1)	0.81, t (12.1)	0.81, t (12.0)	0.80, t (12.1)
2	4.12, m	4.23, m	4.15, m	4.13, m	4.15, m
3α	2.32, dt (11.9, 2.6)	2.40, dt (11.9, 2.7)	2.35, m	2.33, dt (12.5, 2.6)	2.60, dd (12.5, 4.6)
3β	1.24, td (11.9, 5.4)	1.18, td (11.9, 5.4)	1.23, m	1.22, td (12.5, 4.9)	1.32, dd (12.5, 11.2)
4	2.69, m	2.69, m	2.69, m	2.69, m	
5	1.44, m	1.44, m	1.44, m	1.44, m	1.79, m
6α	1.88, m	1.90, m	1.89, m	1.88, m	1.85, m
6β	1.64, m	1.64, m	1.65, m	1.64, m	1.67, m
7α	1.73, dt (13.3, 3.0)	1.74, dt (13.3, 3.1)	1.74, dt (13.3, 3.2)	1.73, dt (13.3, 2.9)	1.65, m
7β	1.42, m	1.43, m	1.44, m	1.43, m	1.44, m
9	1.03, brd (8.0)	1.03, brd (8.1)	1.04, brd (8.0)	1.03, brd (8.0)	1.12, brd (7.7)
11α	1.56, m	1.54, m	1.56, m	1.55, m	1.63, m
11β	1.41, m	1.42, m	1.41, m	1.40, m	1.49, m
12α	1.56, m	1.56, m	1.56, m	1.55, m	1.63, m
12β	1.48, m	1.47, m	1.48, m	1.48, m	1.49, m
13	2.73, m	2.74, m	2.74, m	2.73, m	2.71, m
14α	1.83, brd (11.5)	1.85, brd (11.5)	1.84, brd (11.6)	1.82, brd (11.5)	1.87, m
14β	1.38, dd (11.5, 5.7)	1.39, dd (11.5, 5.7)	1.39, dd (11.6, 4.8)	1.38, dd (11.5, 5.2)	1.39, dd (11.6, 4.9)
15	3.80, s	3.80, s	3.81, s	3.80, s	3.78, s
16					
17a	5.21, brs	5.21, brs	5.22, brs	5.21, brs	5.18, brs
17b	5.07, brs	5.08, brs	5.08, brs	5.08, brs	5.08, brs
20	0.96, s	0.96, s	0.97, s	0.95, s	1.01, s
1′	4.50, d (8.1)	4.58, d (8.0)	4.51, d (8.0)	4.52, d (8.0)	4.68, d (8.1)
2′	4.90, dd (9.3, 8.1)	4.96, dd (9.1, 8.0)	4.99, dd (9.1, 8.0)	4.93, dd (9.4, 8.0)	4.84, dd (9.6, 8.1)
3′	3.60, dd (9.3, 8.5)	3.86, dd (9.3, 9.1)	3.83, dd (9.3, 9.1)	3.79, dd (9.4, 9.1)	4.00, dd (9.6, 9.1)
4′	3.54, dd (9.4, 8.5)	4.90, dd (9.7, 9.3)	4.97, dd (9.7, 9.3)	4.95, dd (9.8, 9.1)	4.90, dd (10.2, 9.1)
5′	3.51, m	3.51, m	3.67, m	4.12, m	3.80, ddd (10.2, 5.3, 2.2)
6′a	4.45, dd (11.8, 1.9)	3.69, dd (12.4, 2.5)	4.18, dd (12.3, 5.0)	4.17, dd (11.2, 4.9)	4.23, dd (12.2, 5.3)
6′b	4.23, dd (11.8, 5.8)	3.62, dd (12.4, 5.9)	4.15, dd (12.3, 2.8)	4.15, dd (11.2, 2.0)	4.12, dd (12.2, 2.2)
1″	4.42, d (7.5)	4.49, d (5.2)	4.50, d (5.4)	4.44, d (5.5)	4.58, d (6.9)
2″	5.19, dd (9.9, 7.5)	4.95, dd (7.7, 5.2)	4.79, dd (7.7, 5.4)	4.98, dd (7.7, 5.5)	4.94, dd (9.3, 6.9)
3″	4.97, dd (9.9, 3.5)	4.97, dd (7.7, 3.3)	3.78, dd (7.7, 3.5)	4.85, dd (7.7, 3.5)	5.02, dd (9.3, 3.5)
4″	5.25, m	5.18, m	5.00, m	4.00, m	5.20, m
5″a	4.04, dd (13.2, 2.7)	3.95, dd (12.5, 5.3)	3.97, dd (12.5, 5.5)	3.88, dd (12.1, 5.3)	3.93, dd (13.1, 3.4)
5″b	3.67, dd (13.2, 1.4)	3.54, dd (12.5, 2.5)	3.50, dd (12.5, 2.8)	3.50, dd (12.1, 2.5)	3.72, dd (13.1, 1.9)
2‴a	2.22, dd (14.9, 7.2)	2.24, dd (14.9, 7.1)	2.27, dd (15.1, 7.1)	2.25, dd (15.2, 6.9)	2.31, dd (15.1, 7.4)
2‴b	2.19, dd (14.9, 7.0)	2.20, dd (14.9, 7.2)	2.22, dd (15.1, 7.1)	2.19, dd (15.2, 7.2)	2.28, dd (15.1, 6.8)
3‴	2.10, m	2.10, m	2.13, m	2.10, m	2.10, m
4‴	0.99, d (6.7)	0.98, d (6.7)	0.99, d (6.6)	0.97, d (6.7)	0.99, d (6.7)
5‴	0.98, d (6.6)	0.97, d (6.6)	0.98, d (6.6)	0.97, d (6.6)	0.99, d (6.6)
4′-OAc		2.06, s	2.02, s	2.02, s	1.96, s
6′-OAc	2.05, s		2.06, s	2.06, s	2.05, s
2″-OAc	2.04, s	2.04, s	2.10, s	2.04, s	2.02, s
3″-OAc	2.00, s	2.03, s		2.06, s	2.10, s
4″-OAc	2.13, s	2.09, s	2.13, s		2.05, s

[a] Data were measured in $CDCl_3$. [b] Data were measured in methanol-d_4.

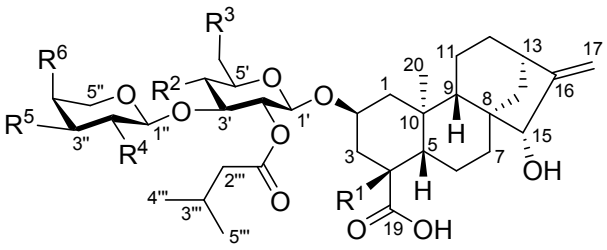

	R^1	R^2	R^3	R^4	R^5	R^6
1	H	OH	OH	OAc	OH	OAc
2	H	OH	OAc	OAc	OH	OAc
3	H	OH	OAc	OAc	OAc	OH
4	H	OAc	OH	OAc	OH	OAc
5	H	OAc	OH	OAc	OAc	OH
6	H	OAc	OAc	OAc	OH	OH
7	H	OH	OAc	OAc	OAc	OAc
8	H	OAc	OH	OAc	OAc	OAc
9	H	OAc	OAc	OAc	OH	OAc
10	H	OAc	OAc	OAc	OAc	OH
11	CO_2H	OAc	OAc	OAc	OAc	OAc

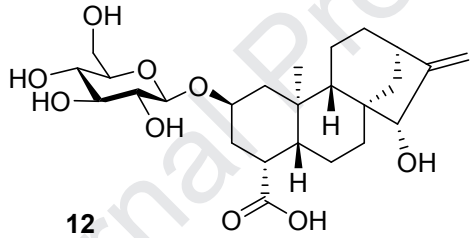

12

Fig. 1. Structures of compounds **1**–**12**.

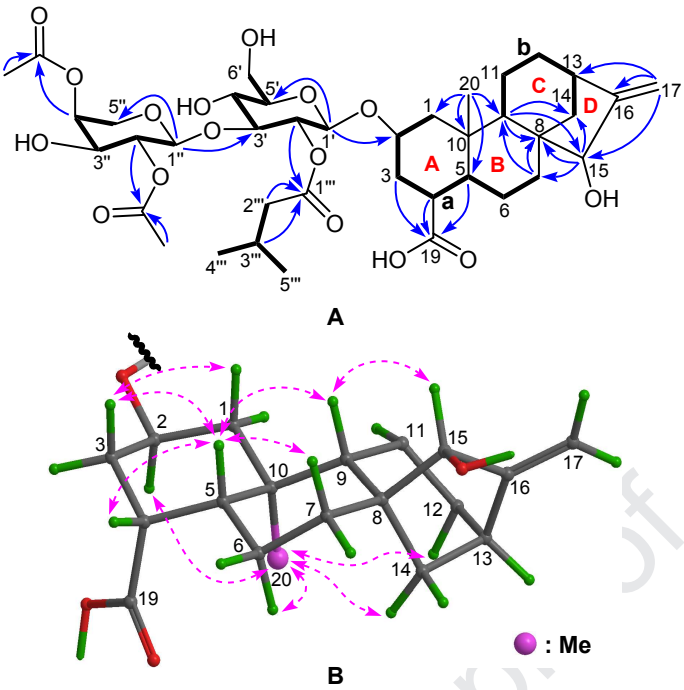

Fig. 2. Key ^{1}H–^{1}H COSY (▬), HMBC (⟶) and ROESY (⇢) correlations for **1** (for clarity, H-11β and H-12β were not shown).

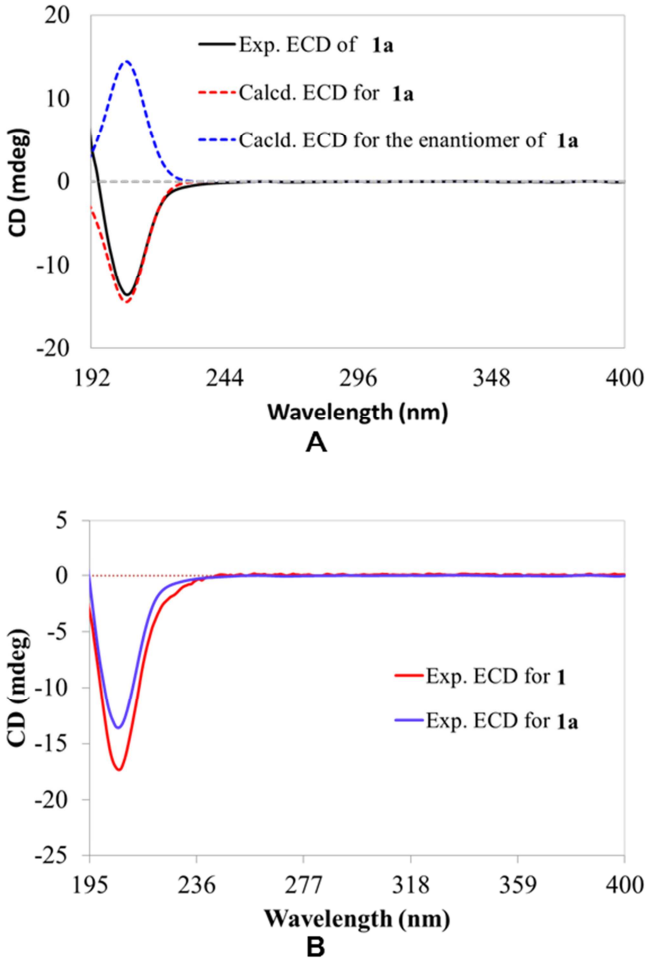

Fig. 3. Experimental and calculated ECD spectra for **1a**, and experimental ECD spectrum for **1**.

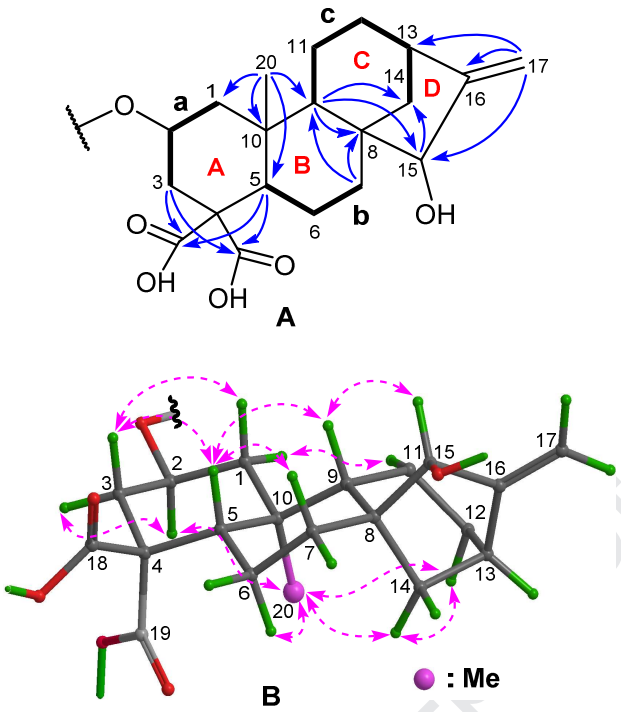

Fig. 4. Key ^{1}H–^{1}H COSY (—), HMBC (⟶) and ROESY (⇢) correlations for **11**.

Highlights

1. Eleven unusual 18-norditerpenoid glycosides were isolated from the flowers of *Inula japonica.*
2. The absolute configurations were determined via chemical derivatization, enzymatic hydrolysis and ECD analysis.
3. An intact diterpenoid glycoside with 4-geminal carboxyl groups showed moderate antibacterial activity.
4. The discovery of these compounds enriches the chemical diversity of metabolites from *Inula* species.